Journal of Science and Transport Technology
Journal homepage: https://jstt.vn/index.php/en

Optimization of the Transmission Ratio in a Two-Stage Spur-Helical Gearbox Using Sequential Quadratic Programming Algorithm

Nguyen Huu Loc[1,2,*], Huynh Hoang Linh[1,2,3], Huynh Huu Duy[1,2]
[1]Faculty of Mechanical Engineering, Ho Chi Minh City University of Technology (HCMUT), 700000 Ho Chi Minh City, Vietnam
[2]Vietnam National University-Ho Chi Minh City, 700000 Ho Chi Minh City, Vietnam
[3]Faculty of Automotive Engineering, Cao Thang Technical College, 700000 Ho Chi Minh City, Vietnam

Article info
Type of article:
Original research paper

DOI:
https://doi.org/10.58845/jstt.utt.2026.en.6.2.388-408

***Corresponding author:**
Email address:
nhloc@hcmut.edu.vn

Received: 17/11/2025
Received in Revised Form: 04/04/2026
Accepted: 29/05/2026

Abstract: Two-stage gear reducers are widely used in industrial power transmission systems due to their ability to reduce speed, increase torque, and maintain high mechanical efficiency. This study proposes a standards-based optimization framework for two-stage gearboxes that simultaneously ensures contact fatigue strength, adequate oil-bath lubrication, and minimized gearbox volume. The optimization problem is formulated analytically and solved using the Sequential Quadratic Programming (SQP) algorithm. The main objective is to establish a practical lookup table for optimal transmission ratio ranges, enabling efficient preliminary design selection. The proposed approach improves computational efficiency while maintaining the physical interpretability of the design variables and constraints. To the best of the authors' knowledge, this study is among the first to simultaneously integrate uniform contact strength, lubrication constraints, and volume minimization within a unified SQP-based optimization framework. The results provide a useful reference for preliminary gearbox design and can support rapid parameter selection in engineering practice, although further adjustments may be required to account for manufacturing constraints and specific operating conditions.

Keywords: Two-stage gearbox, SQP, Optimization, Uniform contact strength, Oil-bath lubrication, Minimum volume.

Nomenclature

Symbols	Units	Description
a_w	mm	center distance
b_w	mm	gear face width
d_{wi}, d_{wj}	mm	pitch circle diameter of driving and driven gears
Z_M		the elasticity factor (material parameter)
v	m/s	pitch line velocity
V	mm^3	volume of two-stage gearbox
n	rpm	rotational speed
K_{as}, K_{ah}		center distance coefficient

Symbols	Units	Description
K_H, K_F		load factor for contact stress and bending stress
m	mm	module of spur gear and normal module of helical gear
P	kW	transmitted power
T_i, T_j	Nm	torque on driving and driven gears
u_{ij}		transmission ratio of each stage
u_h		total transmission ratio
z_i, z_j		number of teeth on driving and driven gears
Z_ε		face load factor
Z_H		geometry factor for contact stress
β	deg	helix angle
α	deg	pressure angle
ψ_{ba}		face-width factor
σ_H	MPa	calculated hertzian contact stress
$[\sigma_H]$	MPa	allowable hertzian contact stress
K_{ds}, K_{dh}		this value depends on the pressure angle, contact ratio, and the material properties of the gears
Abbreviations		
SQP		Sequential Quadratic Programming

1. Introduction

Gear transmissions play a pivotal role across various industrial sectors due to their reliable operation, high efficiency, and large load-carrying capacity. Numerous gear arrangement configurations exist, as illustrated in Fig. 1. The development trend of gear transmissions emphasizes geometric optimization, noise and vibration reduction, and extended service life, while also integrating digital technologies such as CAE simulation, artificial intelligence [1, 2], advanced materials [3] (e.g., wear-resistant alloys, engineering polymers), and high-precision manufacturing via CNC machining or 3D printing [4]. Consequently, modern gear systems not only meet the demands for durable performance but also align well with advanced mechatronic systems, such as robotics and renewable energy equipment.

Over the past decades, design optimization aimed at minimizing the mass and volume of gear transmission systems has attracted considerable attention from researchers. Gologlu and Zeyveli [5] developed an approach based on the genetic algorithm (GA) to automate the preliminary design of gear drives, with the primary objective of minimizing material volume. In that study, the design constraints were mainly centered on the bending stress and contact stress of the helical gear system. Similarly, Sanghvi et al. (2014) [6] performed a multi-objective optimization of a two-stage helical gear system to minimize volume and maximize load-carrying capacity. The study compared three methods: the MATLAB optimization toolbox, the basic GA algorithm, and the NSGA-II algorithm. The results showed that NSGA-II provided the most superior solution in handling conflicting objectives, achieving a 13.08% reduction in volume while increasing load-carrying capacity by 1%, thereby overcoming the shortcomings of conventional nonlinear programming techniques in converging to local minima. Advancing further, Buiga and Tudose (2014) [7] have pointed out a major limitation of previous research, which often focused on optimizing individual components rather than considering the entire system. To address this issue, they applied a genetic algorithm to minimize the mass of a complete two-stage coaxial helical gearbox, including the gears, shaft assemblies, and even the housing. Their model explored a vast design space with 17 mixed design variables and 76 complex nonlinear constraints, thereby achieving a mass reduction of up to 17.94% compared with traditional design methods, while also clearly analyzing the trade-off between mass

reduction and system lifetime. Most recently, Yamanaka et al. [8] proposed a multi-task gearbox optimization (MGO) method based on the gravitational particle swarm algorithm (GPSA), which enables the simultaneous design of multiple feasible gearbox configurations to reduce volume and weight while satisfying up to 11 strength-related constraint conditions.

To meet the stringent requirements of modern transmission systems, research has shifted toward multi-objective optimization, balancing size, efficiency, and noise-vibration characteristics (NVH). Deb and Jain (2003) [9] were among the pioneers in applying the NSGA-II to the design of multi-speed gearboxes. Unlike classical methods, which often require the problem to be decomposed into independent subproblems, NSGA-II is capable of directly handling multi-objective problems with mixed variables (discrete and continuous) without the need for complex penalty parameters. That study demonstrated its effectiveness in identifying multiple Pareto-optimal solutions in a single run, while simultaneously optimizing material mass, power transmission capacity, center distance, and output speed error. Following this direction, Kim et al. (2020) [10] used the NSGA-III algorithm to optimize the macro-geometry of a helical gear pair, considering three objectives: mass, efficiency, and peak-to-peak static transmission error (PPSTE) - a major cause of noise and vibration. Building on this success, in 2025, Kim's group [11] proposed an optimal design strategy integrating both macro- and micro-geometry through a two-stage optimization process to minimize power loss and PPSTE while still ensuring safety factors for strength. By using a Random Forest regression model to analyze the results, they extracted the core macro-geometric parameters, which enabled a reduction of 38–77% in PPSTE and 36–58% in gear mesh loss when micro-optimization was integrated. Along the same line of integrated NVH-oriented optimization, Kalligeros et al. (2026) [12] developed a macro-geometry optimization procedure to improve the weight, efficiency, and NVH characteristics of spur gears. The key innovation of this study lies in the application of a feedforward neural network (FFNN) to rapidly predict the static transmission error curve, thereby reducing vibration, decreasing power loss by up to 40%, and lowering the RMS value of dynamic transmission error (DTE) by more than 35%. Furthermore, previous studies by O. Buiga et al. [13], B. Karmi et al. [14], and M. Patil et al. [15] have confirmed the effectiveness of optimization algorithms in reducing gearbox size and enhancing performance.

In addition to the optimization of macro-geometric parameters, many studies have examined the mechanical nature of gears in greater depth. Sánchez et al. (2019) [16] developed an advanced strength model to calculate bending stress and surface pitting for internal spur gears in mesh. This model determines the load-sharing ratio among simultaneously contacting tooth pairs based on mesh stiffness, while fully accounting for bending, compressive, shear, and Hertzian deformations. From a dynamic perspective, Wang et al. (2020) [17] developed an improved computational method to predict the vibration response and noise radiation of a two-stage gearbox, in which shaft flexibility and the time-varying stiffness of the bearings were taken into consideration.

Based on the development of existing studies, it is evident that gearbox optimization methods have achieved significant progress, particularly through the application of evolutionary algorithms (e.g., GA and NSGA-II) and machine learning techniques to reduce volume and mass, as well as to improve efficiency and dynamic NVH performance. However, these approaches still exhibit several fundamental limitations when applied to practical engineering design.

First, regarding strength distribution, most existing studies treat bending and contact stresses as minimum safety constraints to prevent failure.

This approach does not account for differences in service life between gear stages and lacks a mechanism to ensure uniform strength distribution. As a result, optimized designs may lead to unbalanced configurations, where some gear stages are overdesigned while others operate close to their failure limits.

Second, regarding lubrication conditions, although lubrication failure is widely recognized as a critical factor leading to surface damage such as wear, pitting, and scuffing, it is often neglected in optimization formulations. Existing approaches rarely incorporate operating conditions to ensure adequate lubrication performance throughout the design process.

Therefore, in the preliminary design stage, the absence of a unified framework capable of simultaneously integrating (i) uniform strength distribution, (ii) lubrication constraints, and (iii) volume minimization remains a critical challenge for gearbox designers. Addressing this gap would not only improve design reliability and durability but also provide a more balanced and efficient transmission system.

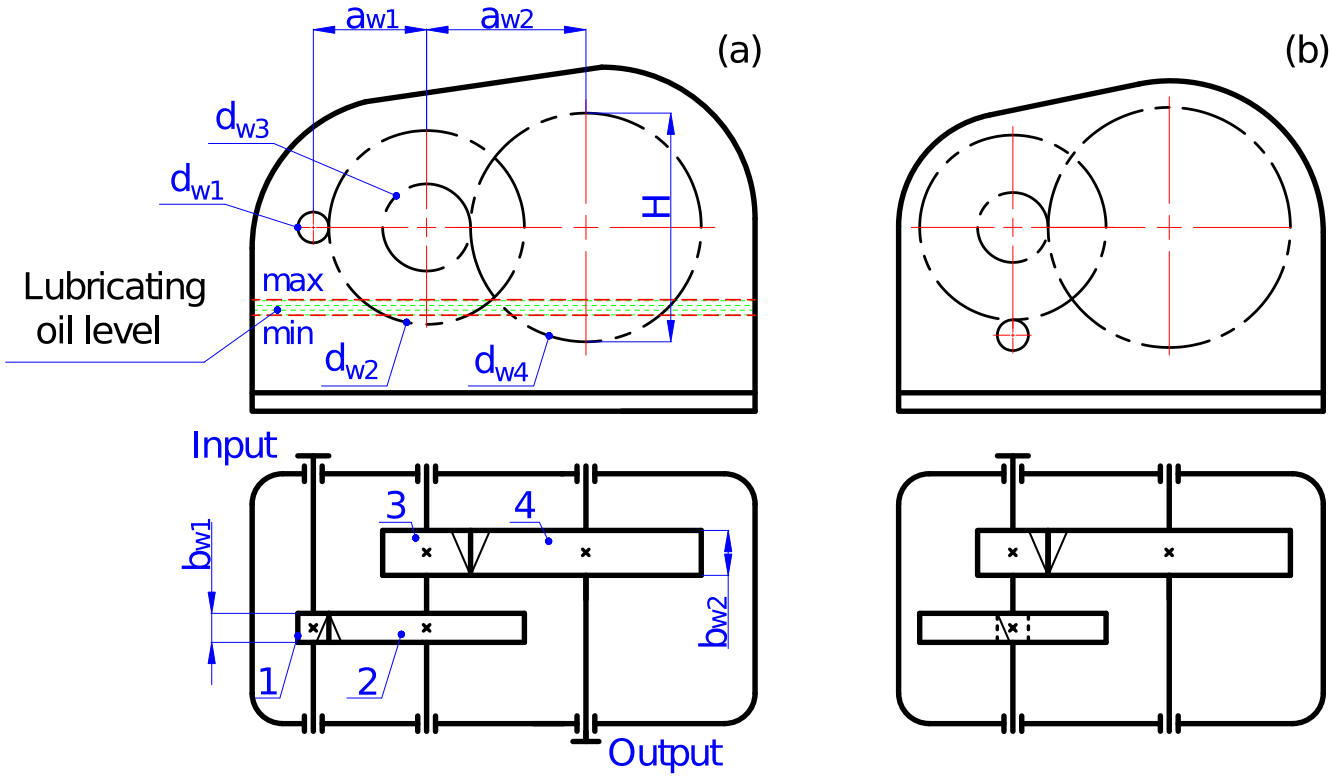

Fig. 1. Configurations of two-stage gearbox layouts (a) in the same plane and (b) in the orthogonal plane layouts

To address this issue, the present study focuses on the geometric optimization of a two-stage gearbox with different layout configurations (Fig. 1). The objective is to determine the optimal transmission ratio distribution for each stage under the constraints of uniform contact strength, oil-bath lubrication, and minimum gearbox volume. These constraints are formulated analytically, and the optimization problem is solved using the Sequential Quadratic Programming (SQP) algorithm. The results are further used to construct a practical lookup table for preliminary design selection.

Within this scope, the study is limited to the preliminary design stage and does not consider detailed design aspects such as vibration, noise, material selection, thermal effects of lubricants, or manufacturing constraints. Therefore, the proposed results are intended to support initial design decisions rather than final engineering

validation.

To the best of the authors' knowledge, this study is among the first to simultaneously integrate uniform contact strength, lubrication constraints, and volume minimization within a unified SQP-based optimization framework. By combining standards-based analytical formulations with an efficient optimization strategy, the proposed approach provides a physically interpretable and computationally efficient tool for gearbox design.

2. Mathematical Formulation

2.1. Ensuring Uniform Contact Strength

For well-lubricated gear transmissions, the dominant failure mode is surface pitting [18], and the design should therefore be based on the contact fatigue strength, denoted as σ_H. To reduce material usage, the design should ensure uniform contact strength across all gear pairs. The problem of allocating the transmission ratios within the gear system, while satisfying both the uniform contact strength and the oil-lubrication condition, is considered an optimization problem. This problem is formulated through the distribution of transmission ratios $\mathbf{X}$ among the gear pairs, and is defined as follows:

$$\mathbf{X} = \begin{bmatrix} u_{12} \\ u_{34} \\ \dots \\ u_{i,j} \end{bmatrix} \quad (1)$$

To ensure uniform contact strength, the contact stress values between all gear pairs must be equal, as follows:

$$\sigma_{H12} \approx \sigma_{H34} \approx \dots \approx \sigma_{Hij} \quad (2)$$

In the calculation of contact stress for spur and helical gears, the commonly referenced standard methods include ISO 6336-2:2006, ANSI/AGMA 2101-E25, and DIN 3990-2:1987-12. Among these, ISO 6336-2:2006 [19] provides the fundamental equations for determining surface load capacity and evaluating the contact durability (pitting) of external or internal involute cylindrical gears, mainly for oil-lubricated gear transmissions. Similarly, ANSI/AGMA 2101-E25 [20] provides a method for evaluating the macropitting resistance and bending strength of involute spur and helical gear pairs, whereas DIN 3990-2:1987-12 [21] focuses on the calculation of pitting resistance of cylindrical gears. Although multiple standard systems are available, this study uses only ISO 6336-2:2006 to calculate contact stress in order to ensure consistency with the theoretical basis, calculation factors, and evaluation procedure throughout the entire research model. The contact stress between gear pairs (i; j) is determined by the following equation. Alternatively, the formula for determining the contact stress can be found in [19, 22].

$$\sigma_{Hij} = Z_{Mi} Z_{Hi} Z_{\varepsilon i} \sqrt{\frac{2T_i \cdot 10^3 \cdot K_{Hij}(u_{ij}+1)}{d_{wi}^2 b_{wi} u_{ij}}} \le [\sigma_{Hij}] \quad (3)$$

Where [22]:

$$d_{wj} = \frac{2 b_{wi} u_{ij}}{\psi_{baij}(u_{ij}+1)} \cos\beta \quad (4)$$

$$b_{wi} = \frac{\psi_{baij} d_{wj}(u_{ij}+1)}{2u_{ij}} = \psi_{baij} a_{wij} \quad (5)$$

In this study, only two-stage gear transmissions are considered. Therefore, to ensure uniform contact strength, the following condition must be satisfied:

$$\sigma_{H12} = \sigma_{H34} \quad (6)$$

From equations (3)-(6), it follows that:

$$u_{12} = \frac{u_h \left(\frac{a_{w12}}{a_{w34}}\right)^3 \sqrt{\left(\frac{K_{as}}{K_{ah}}\right)^2 \frac{\psi_{ba12}}{u_h \psi_{ba34}} - 1}}{1 - \left(\frac{a_{w12}}{a_{w34}}\right)^3 \sqrt{\left(\frac{K_{as}}{K_{ah}}\right)^2 \frac{\psi_{ba12}}{u_h \psi_{ba34}}}} \quad (7)$$

Where [19, 22, 23]: $K_{as} = 500$ for spur gears; $K_{ah} = 430$ for helical gears.

The contact stress in a two-stage gearbox with orthogonal plane layout, as shown in Fig.1(b) is analogous to that of the horizontally expanded two-stage gearbox and is also calculated using

equation (7).

2.2. Ensuring Oil-Bath Lubrication Conditions

In enclosed gearboxes that are regularly maintained, the primary lubrication method is oil-bath lubrication [24]. Oil-bath lubrication is a method in which the rotating gears splash oil onto the meshing surfaces, forming a film that reduces friction, wear, and dissipates heat, thereby extending the service life of the gearbox [25]. This method features a simple design and low cost. However, its effectiveness depends on the oil level and gear speed; if not properly optimized, it may lead to hydraulic losses or insufficient lubrication. During operation, the gearbox must maintain complete sealing; if oil splashes out or the oil level drops, the meshing zone will lack lubrication and may be damaged.

This method is suitable when the pitch-line velocity does not exceed $12\ \mathrm{m/s}$ ($v \le 12\ \mathrm{m/s}$) [22, 24, 26]. If the velocity exceeds this limit, the oil is excessively agitated, which reduces transmission efficiency, promotes foaming, entrains air, and accelerates oxidation, thereby diminishing the lubricant's effectiveness [22, 24].

For multi-stage gearboxes, the driven gears should be immersed in oil; if this is not feasible, an auxiliary gear may be added to splash oil onto the meshing region [24]. The oil immersion depth for immersed gears must not be less than 10 mm from addendum circle diameter of the gear [24], and for the largest gear, the immersion depth may reach up to 1/6 of its diameter [24]. If the pitch-line velocity is extremely low, the immersion depth may even reach up to half of the gear diameter.

2.2.1. Two-Stage Gearbox with Same Plane Layout

To ensure proper lubrication conditions, the pitch circle diameters of the driving and driven gears in each gear pair ($d_{w2}; d_{w4}$) must satisfy the following condition:

$$\frac{2}{3}d_{w4} \le d_{w2} \le d_{w4} \tag{8}$$

Based on the formulas for calculating the geometric parameters of gears provided in [22], it follows that:

$$d_{wj} = K_{dsj}\sqrt[3]{\frac{2T_i K_{Hi} u_{ij}^2}{\psi_{baij}[\sigma_{Hij}]^2}} \tag{9}$$

Where [19, 22, 23]: $K_{ds} = 756$ for spur gears; $K_{ds} = 680$ for helical gears.

If both gear pairs are either helical or spur, then $K_{H12} \approx K_{H34}$. From equations (5), (8), and (9), it follows that:

$$\frac{2}{3}\sqrt[3]{\frac{\psi_{ba12}[\sigma_{H12}]^2 u_h^2}{\psi_{ba34}[\sigma_{H34}]^2}} \le u_{12} \le \sqrt[3]{\frac{\psi_{ba12}[\sigma_{H12}]^2 u_h^2}{\psi_{ba34}[\sigma_{H34}]^2}} \tag{10}$$

2.2.2. Two-Stage Gearbox with Orthogonal Plane Layout

The oil-bath lubrication condition for the gearbox in this configuration is established as follows:

$$\frac{2}{3}d_{w4} \le 2(d_{w1} + 0.5d_{w2}) \le d_{w4} \tag{11}$$

From equations (5), (9), and (11), it follows that:

$$\frac{2}{3}\cdot\frac{K_{ds}}{K_{dh}}\sqrt[3]{\frac{\psi_{ba12}[\sigma_{H12}]^2 K_{H34} u_h^2}{\psi_{ba34}[\sigma_{H34}]^2 K_{H12}}} - 2 \le u_{12} \le \frac{K_{ds}}{K_{dh}}\sqrt[3]{\frac{\psi_{ba12}[\sigma_{H12}]^2 K_{H34} u_h^2}{\psi_{ba34}[\sigma_{H34}]^2 K_{H12}}} - 2 \tag{12}$$

2.3. Ensuring Minimum Volume

2.3.1. In the Same Plane

Objective: To determine the transmission ratio u_{12} that minimizes the gearbox volume.

Objective function: $V_1(u_{12})_{min}$

The volume V is determined based on Fig. 1(a), as follows:

$$V_1 = L_1 \cdot B_{w1} \cdot H_1 \tag{13}$$

Where: $L_1 = a_{w1} + a_{w2} + 0.5d_{w1} + 0.5d_{w4}$; $B_{w1} = b_{w1} + b_{w3}$; $H_1 = d_{w4}$

The center distance a_{wi} is determined using the formula provided in [19, 22, 23] as follows:

$$a_{wij} = K_{asi}\sqrt[3]{\frac{T_i K_{Hi}\left(u_{ij}+1\right)^3}{\psi_{baij}\left[\sigma_{Hij}\right]^2 u_{ij}}} \quad (14)$$

From equations (4), (5), (13), and (14), it follows that: (15)

Where:

$$A_1 = 2K_{as1}^2 K_{as3}\sqrt[3]{\frac{\psi_{ba12}K_{H\beta1}^2 K_{H\beta3}}{\psi_{ba34}[\sigma_{H12}]^4[\sigma_{H34}]^2}}$$

$$B_1 = 2K_{as1}K_{as3}^2\sqrt[3]{\frac{\psi_{ba12}^2 K_{H\beta1}^2 K_{H\beta3}}{\psi_{ba34}^2[\sigma_{H12}]^2[\sigma_{H34}]^4}}$$

$$C_1 = 2K_{as1}K_{as3}^2\sqrt[3]{\frac{\psi_{ba34}K_{H\beta1}^2 K_{H\beta3}}{\psi_{ba12}[\sigma_{H12}]^2[\sigma_{H34}]^4}}$$

$$D_1 = 2K_{as3}^3\left(\frac{K_{H\beta3}}{[\sigma_{H34}]^2}\right)$$

To solve the optimization problem, the derivative of equation (15) is taken $\frac{dV_1}{du_{12}} = 0$. The resulting expression is as follows: (16)

2.3.2. In the Orthogonal Plane

The calculation is similar to the volume equation (13) applied to Fig. 1(b), but with the coefficients defined as $L_2 = a_{w2} + 0.5d_{w2} + 0.5d_{w4}$

By simplifying the volume expression, we obtain the following equation: (17)

Where:

$$A_2 = 2K_{as1}K_{as3}^3\sqrt[3]{\frac{\psi_{ba12}^2 K_{H\beta1}K_{H\beta3}^2}{\psi_{ba34}^2[\sigma_{H12}]^2[\sigma_{H34}]^4}}$$

$$B_2 = 2K_{as3}^3\left(\frac{K_{H\beta3}}{[\sigma_{H34}]^2}\right)$$

$$C_2 = 2K_{as1}^2 K_{as3}\sqrt[3]{\frac{\psi_{ba12}K_{H\beta1}^2 K_{H\beta3}}{\psi_{ba34}[\sigma_{H12}]^4[\sigma_{H34}]^2}}$$

$$D_2 = 2K_{as1}^2 K_{as3}\sqrt[3]{\frac{\psi_{ba34}K_{H\beta1}^2 K_{H\beta3}}{\psi_{ba12}[\sigma_{H12}]^2[\sigma_{H34}]^4}}$$

To solve the optimization problem, the derivative of equation (17) is taken $\frac{dV_2}{du_{12}} = 0$. The resulting expression is as follows:

$$u_{12} = \sqrt{\frac{\left(2A_2\sqrt[3]{u_h^4} + 2B_2u_h^2\right)}{C_2\sqrt[3]{u_h^2} + (A_2+D_2)\sqrt[3]{u_h} + B_2}} \quad (18)$$

$$V_1(u_{12}) = T_I\left(\left(A_1\sqrt[3]{u_h^2} + B_1\sqrt[3]{u_h} + C_1\sqrt[3]{u_h} + D_1\right)u_{12} + \left(2A_1\sqrt[3]{u_h^2} + 2B_1\sqrt[3]{u_h^4} + 2C_1\sqrt[3]{u_h^4} + 2D_1u_h^2\right)\left(\frac{1}{u_{12}}\right) + 2B_1\sqrt[3]{u_h^4} + C_1\sqrt[3]{u_h^4} + 3D_1u_h + 3A_1\sqrt[3]{u_h^2} + B_1\sqrt[3]{u_h} + 2C_1\sqrt[3]{u_h}\right) \quad (15)$$

$$u_{12} = \sqrt[2]{\frac{2\left(A_1\sqrt[3]{u_h^2} + (B_1+C_1)\sqrt[3]{u_h^4} + D_1u_h^2\right)}{A_1\sqrt[3]{u_h^2} + (B_1+C_1)\sqrt[3]{u_h} + D_1}} \quad (16)$$

$$V_2(u_{12}) = T_I\left(\left(A_2\sqrt[3]{u_h} + B_2 + C_2\sqrt[3]{u_h^2} + D_2u_h\sqrt[3]{\frac{1}{u_h^2}}\right)u_{12} + \left(2A_2\sqrt[3]{u_h^4} + 2B_2u_h^2\right)\frac{1}{u_{12}} + 2A_2\sqrt[3]{u_h^4} + D_2\sqrt[3]{u_h^4} + C_2\sqrt[3]{u_h^2} + A_2\sqrt[3]{u_h} + 3B_2u_h\right) \quad (17)$$

3. Optimization Using the SQP Algorithm

3.1. SQP Algorithm

In recent years, the two main algorithmic approaches commonly used to solve this problem are: derivative-based algorithms, such as SQP, and derivative-free evolutionary algorithms, such as GA or NSGA-II.

Many studies have successfully applied these algorithms. Typically, Bozca (2018) [27] used the SQP algorithm to optimize the geometric parameters of a gearbox in order to minimize transmission error and rattle noise, while satisfying the constraints on contact stress and bending stress. Xu and Min (2013) [28] also successfully applied SQP through the MATLAB toolbox to optimize the volume of a gear drive with high accuracy and efficiency. In another aspect, evolutionary algorithms such as GA are often highly regarded for their ability to avoid local minima and to work well with discrete variables. However, in a comprehensive comparison between SQP and GA, Chaturvedi et al. (2023) [29] pointed out that GA requires a significant computational cost compared with SQP. Similarly, Elsiedy et al. (2024) [30], when studying multi-objective optimization for plastic gears, had to combine GA with SQP into a hybrid approach, in which SQP played the core role in local search to achieve the fastest and most accurate convergence.

The choice of the SQP algorithm, instead of evolutionary algorithms (GA or NSGA-II), is determined based on the characteristics of the continuous-variable geometric optimization problem. This decision is reinforced by the following three decisive advantages:

First, in terms of computational efficiency and time cost, SQP directly exploits derivative (gradient) information to determine the search direction toward the minimum, making this algorithm computationally far more efficient than evolutionary algorithms. Meanwhile GA or NSGA-II require the objective function to be evaluated repeatedly tens of thousands of times over populations, resulting in an extremely slow convergence rate. Notably, the research results of Chaturvedi et al. (2023) [29] experimentally demonstrated that, for the macro-geometry optimization of gear structures, SQP required only 7 seconds, whereas GA consumed up to 245 seconds – that is, the computational time of GA was 3400% longer. For this study's problem, optimizing computational performance while still obtaining good results is a top priority.

Second, in terms of absolute accuracy and fast convergence, evolutionary algorithms often carry the risk of premature convergence and high randomness due to their dependence on crossover and mutation parameters. In contrast, the direct solution of the K-T equations makes SQP a local search tool with a fast convergence rate and extremely accurate results. In mechanical engineering, where even the smallest errors can affect system performance, SQP provides maximum design accuracy with highly reliable numerical algorithms.

Third, in terms of suitability for a continuous-variable space and strict nonlinear constraints: In transmission design, the problem must satisfy strict systems of inequality constraints such as the bending stress limit at the tooth root, the contact stress on the surface, and the maintenance of the center distance. The capability of SQP to handle nonlinear constraint penalties is excellent. Although GA has an advantage when the input parameters are forced into discrete variables (for example: enforced selection of standard module, standard center distance, standard transmission ratio, etc.), the problem in this study is defined in a continuous variable space. The use of heuristic methods would introduce excessive complexity and redundant population dispersion.

With continuous search space and stringent requirements on geometric boundary conditions and stress constraints, SQP is the most suitable optimization algorithm for the transmission system in this study, overcoming the limitations of

computational time and accuracy associated with evolutionary algorithms such as GA and NSGA-II.

3.2. Application of the SQP Algorithm to Optimization

SQP is an iterative method for solving nonlinear constrained optimization problems. At each iteration, the original problem is approximated by a QP subproblem, in which the objective function is a second-order Taylor expansion of the Lagrangian, and the constraints are linearized. Specifically, starting from an initial point, SQP computes the gradient and Hessian (or an approximation of the Hessian) of the Lagrangian, constructs and solves the QP subproblem to determine a search direction as illustrated in Fig. 2, then updates the decision variables and Lagrange multipliers. This process is repeated until a stopping criterion is met (e.g., sufficiently small gradient norm or negligible variable changes). By leveraging the second-order structure, SQP achieves superlinear or quadratic convergence near the solution, making it highly effective for problems with smooth objective and constraint functions. As such, it is widely used in applications such as optimal design, mixed control systems, and parameter estimation.

The objective function of the optimization problem is constructed on the basis of three main requirements: (i) ensuring uniform contact strength, (ii) satisfying the oil-bath lubrication condition, and (iii) minimizing the gearbox volume. Accordingly, the objective of the problem is to determine the transmission ratio u_{12} such that all three requirements are simultaneously satisfied. The constraints of the problem are established according to Eqs. (7), (8), (10), (12), (16), and (18). In these equations, the parameters $u_{12}, u_{34}, u_{56}, m, b_w, \psi_{ba}$ and a_w are selected according to their corresponding standard values, while the quantities $z_1, z_2, z_3, \dots, z_n$ are restricted to integers. In addition, the condition of uniform contact fatigue strength is imposed on the gear pairs according to the relation $\sigma_{H12} \approx \sigma_{H34}$, in combination with the constraints stated in Eqs. (4) and (5).

The objective functions and the constraint conditions of the problem are specifically presented as follows:

The objective functions of volumes V_1 and V_2 are presented in Eqs. (15) and (17), respectively.

The constraints:

Contact stress constraint:

$$g_1(x) = \sigma_{Hij} - [\sigma_{Hij}] \le 0 \quad (19)$$

Uniform strength among gear pairs:

$$g_2(x) = \sigma_{H12} - \sigma_{H34} = 0 \quad (20)$$

Oil-bath lubrication:

$$g_3(x) = \frac{2}{3} d_{w4} - d_{w2} \le 0 \quad (21)$$

$$g_4(x) = d_{w2} - d_{w4} \le 0 \quad (22)$$

Standard transmission ratio u_h: (23)

$$g_5(x) = u_h = \begin{Bmatrix} 8;\ 9;\ 10;\ 11.2;\ 12.5;\ 14;\ 16;\ 18;\ 19;\ 20; \\ 22.4;\ 25;\ 28;\ 31.5;\ 35.5;\ 40;\ 45;\ 50 \end{Bmatrix}$$

Standard face-width coefficient ψ_{ba}:

$$g_6(x) = \psi_{ba} = \{0.25; 0.315; 0.4\} \quad (24)$$

The algorithm was implemented in MATLAB using the *fmincon* function in the Optimization Toolbox to solve the constrained nonlinear optimization problem. During the implementation process, it is first necessary to define the objective function, select the initial starting point x0, set the lower bounds lb and upper bounds ub, and construct the nonlinear constraint function nonlcon, in which the inequality constraints are expressed in the form $c(x) \le 0$. Then, the solver is configured using optimoptions, with the 'sqp' algorithm selected in *fmincon*, and the optimization is carried out for each investigated parameter set. In each run, *fmincon* starts from the point x0 and searches for a local minimum solution that satisfies the prescribed constraints. Therefore, the quality of the initial point and the way the constraints are formulated directly affect the convergence capability of the algorithm. In this problem, the same system of constraints is used for two calls to

fmincon: one with the original objective function to determine the minimum value, and one with the sign-inverted objective function to determine the maximum value of the design variable within the feasible domain.

The implementation procedure of the optimization algorithm using the fmincon function with the SQP method is summarized in the flowchart in Fig. 2.

4. Results and Discussion

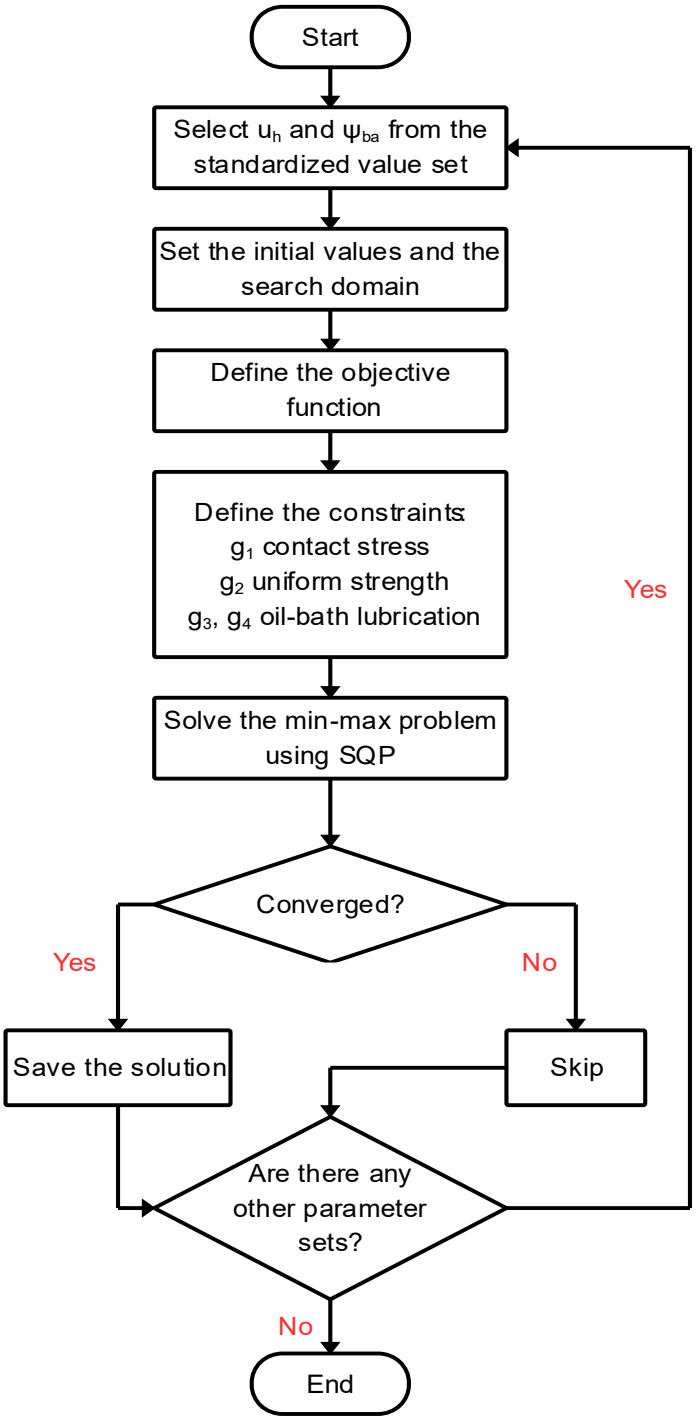

Fig. 2. Main flowchart of the SQP algorithm

In this study, several fundamental assumptions are established as follows: the gearbox operates under constant load and speed, the viscosity of the lubricant is considered unchanged throughout operation, the transmission system is assumed to be a sealed gearbox with

adequate lubrication and no oil leakage, the transmission efficiency is taken as constant; and both gearbox configurations spur gears arranged in the same plane and spur gears arranged in an orthogonal plane are evaluated under the same power rating and identical operating conditions. Design parameters such as transmission ratio, face width, face-width coefficient, and center distance are selected according to standardized series values to ensure practicality and consistency in both design and manufacturing.

The standardized coefficients used in the calculations are selected as follows:

The face-width coefficients for spur gears follow the standardized series [23, 31]: 0.1; 0.125; 0.16; 0.2; 0.25; 0.315; 0.4; 0.5; 0.63; 0.8; 1.00; 1.25. In this study, the selected values are $\psi_{ba34} = \{0.25; 0.315; 0.4\}$.

The overall transmission ratio u_h follows the standardized series [23, 31] : 1.0; 1.12; 1.25; 1.4; 1.6; 1.8; 2.0; 2.24; 2.5; 2.8; 3.15; 3.55; 4.0; 4.5; 5.0; 5.6; 6.3; 7.1; 8.0; 9.0; 10.0; 11.2; 12.5; 14.0; 16.0; 18.0; 20.0; 22.4; 25; 28; 31.5; 35.5; 40.0; 45.0; 50.0; 56.0; 63.0; 71.0; 80.0; 90.0; 100; 112; 125; 140; 160; 180; 200; 224; 250; 280; 315; 355; 400; 450; 500; ...

According to the number of stages, the maximum overall transmission ratio of a gear reducer increases significantly as the number of stages rises. Specifically, for a single-stage gear reducer, the overall transmission ratio generally does not exceed $u_h \leq 6$; in some cases, it may reach $u_h \leq 8$; and at the extreme limit, it may be as high as $u_h \leq 18$ [22]. For a two-stage gear reducer, the overall transmission ratio is generally limited to $u_h \leq 35$, may reach $u_h \leq 45$, and can attain a maximum of $u_h \leq 60$ [22]. For a three-stage gear reducer, the overall transmission ratio generally does not exceed $u_h \leq 150$, may reach $u_h \leq 200$, and in the extreme case may be as high as $u_h \leq 300$ [22, 23]. Thus, when a higher transmission ratio is required, increasing the number of stages becomes necessary to ensure operating capability and design rationality.

However, for two-stage spur gear transmissions, the overall transmission ratio u_h belongs to the standardized subset:

$$u_h = \{8;\ 9;\ 10;\ 11.2;\ 12.5;\ 14;\ 16;\ 18;\ 19;\ 20; 22.4;\ 25;\ 28; 31.5; 35.5; 40; 45; 50\}.$$

For helical gear transmissions, the helix angle β significantly affects the tooth's contact load-carrying capacity. In formula (4), β is typically selected within the range $\beta = 8 \div 20^0$ [19, 22]. According to ISO 6336-2 [19] and [22], the pressure angle α commonly adopts the standardized values of $20^0, 22.5^0, 25^0$. In this study, the pressure angle is selected as $\alpha = 20^0$.

4.1. Analytical Calculation

Based on equations (7), (8), (10), (12) and (15)-(18), together with the aforementioned constraints, the analytical calculation yields the results shown in Table 1.

Table 1 shows that as the overall transmission ratio u_h increases, the minimum value, maximum value, and minimum volume V_{min} all increase across all investigated cases. For the same values of u_h and K, the same-plane layout always gives higher u_{12} values than the orthogonal one, whereas the latter generally results in a smaller minimum volume. In addition, when K rises from 1.25 to 1.6, the feasible range of u_{12} tends to decrease, while V_{min} slightly increases. This indicates that u_{12} is not a fixed value, but rather a design range that depends on the gearbox layout and the selected design parameters.

4.2. Using the SQP Algorithm

Based on equations (7), (10), (15), and (16), SQP algorithm is employed to incorporate the previously defined constraints. The optimization process is carried out using MATLAB, and the results are presented in Table 2.

Table 2 indicates that the feasible range of u_{12} increases progressively with u_h for all

investigated layouts. Similar to the analytical results in Table 1, the same-plane layout always provides higher u_{12} values than the orthogonal one. However, compared with Table 1, the SQP-based results in Table 2 show a wider feasible range of u_{12}, which suggests that the optimization procedure is able to identify a broader design domain. Moreover, increasing K leads to rise in u_{12} in Table 2, which differs from the trend observed in Table 1 and highlights the influence of the optimization model on the obtained transmission ratio distribution.

Overall, the results from Tables 1 and 2 confirm that the transmission ratio distribution of a two-stage gearbox strongly depends on the overall transmission ratio, the gearbox layout, and the ratio K. While Table 1 provides the analytical trend together with the minimum volume, Table 2 displays a broader feasible design range obtained by SQP optimization. Therefore, both tables are useful for preliminary design, with Table 1 serving as an initial analytical reference and Table 2 supporting the selection of optimized parameter ranges.

Based on the data presented in Table 2, MATLAB is used to visualize the parameter values in graphical form for better interpretation and easier reference, as shown in Fig. 3 and Fig. 4.

Table 1. Transmission ratio distribution of a developed two-stage gearbox

u_h	In the same plane						In the orthogonal plane					
	$K=\frac{\psi_{ba34}}{\psi_{ba12}}=1.25$			$K=\frac{\psi_{ba34}}{\psi_{ba12}}=1.6$			$K=\frac{\psi_{ba34}}{\psi_{ba12}}=1.25$			$K=\frac{\psi_{ba34}}{\psi_{ba12}}=1.6$		
	u_{12}			u_{12}			u_{12}			u_{12}		
	min	max	V_{min}	min	max	V_{min}	min	max	V_{min}	min	max	V_{min}
8	2.75	4.13	5.14	2.53	3.80	5.22	0.56	1.85	4.72	0.36	1.54	4.77
9	2.98	4.47	5.56	2.74	4.11	5.66	0.77	2.16	5.14	0.55	1.83	5.21
10	3.19	4.79	5.98	2.94	4.41	6.09	0.98	2.46	5.56	0.74	2.11	5.63
11.2	3.45	5.17	6.46	3.17	4.76	6.58	1.21	2.81	6.05	0.96	2.43	6.13
12.5	3.71	5.56	6.97	3.41	5.12	7.11	1.45	3.18	6.56	1.18	2.77	6.66
14	4.00	6.00	7.54	3.68	5.52	7.69	1.72	3.59	7.13	1.43	3.14	7.25
16	4.37	6.55	8.28	4.03	6.04	8.45	2.07	4.11	7.87	1.75	3.62	8.01
18	4.73	7.09	8.99	4.35	6.53	9.18	2.40	4.61	8.58	2.06	4.08	8.74
19	4.90	7.35	9.33	4.51	6.77	9.53	2.57	4.85	8.93	2.20	4.31	9.10
20	5.07	7.60	9.68	4.67	7.00	9.89	2.72	5.09	9.28	2.35	4.53	9.45
22.4	5.47	8.20	10.48	5.03	7.55	10.71	3.09	5.64	10.08	2.69	5.04	10.29
25	5.88	8.82	11.32	5.42	8.13	11.58	3.48	6.22	10.93	3.05	5.57	11.16
28	6.35	9.52	12.26	5.84	8.76	12.55	3.91	6.87	11.88	3.44	6.17	12.14
31.5	6.86	10.29	13.33	6.32	9.48	13.65	4.39	7.59	12.95	3.89	6.83	13.25
35.5	7.43	11.15	14.51	6.85	10.27	14.86	4.93	8.39	14.14	4.38	7.57	14.47
40	8.05	12.07	15.79	7.41	11.12	16.18	5.50	9.25	15.43	4.91	8.36	15.8
45	8.71	13.06	17.16	8.02	12.03	17.60	6.11	10.17	16.82	5.47	9.21	17.23
50	9.34	14.01	18.50	8.60	12.90	18.98	6.70	11.5	18.16	6.01	10.02	18.62

In the pre-design stage, for two-stage gearboxes whose shaft centerlines lie either in the same plane or in two orthogonal planes with layouts similar to Fig. 1(a) and Fig. 1(b). Table 2 is recommended for the preliminary selection of the first-stage transmission ratio u_{12} and the second-

stage transmission ratio u_{34}, based on the standardized transmission ratio series. When the ratio of the gear face widths between pairs (3;4) and (1;2) is $K = 1.25$ or $K = 1.6$ the face-width coefficient pairs (ψ_{ba12}; ψ_{ba34}) may be selected according to standards as follows: (0,25; 0,315), (0,315; 0,4) or (0,25; 0,4). Alternatively, other combinations of face-width coefficients may also be used, provided that they satisfy the required ratio $K = 1.25$ or $K = 1.6$.

Table 2. Transmission ratio distribution for two-stage gearboxes with expanded layout

u_h	In the same plane				In the orthogonal plane			
	$K = \frac{\psi_{ba34}}{\psi_{ba12}} = 1.25$		$K = \frac{\psi_{ba34}}{\psi_{ba12}} = 1.6$		$K = \frac{\psi_{ba34}}{\psi_{ba12}} = 1.25$		$K = \frac{\psi_{ba34}}{\psi_{ba12}} = 1.6$	
	u_{12}		u_{12}		u_{12}		u_{12}	
	min	max	min	max	min	max	min	max
8	2.87	4.31	3.12	4.54	0.87	2.31	1.12	2.68
9	3.11	4.66	3.37	4.89	1.11	2.66	1.37	3.06
10	3.33	5.00	3.62	5.23	1.33	3.00	1.62	3.43
11.2	3.59	5.39	3.90	5.62	1.59	3.39	1.90	3.85
12.5	3.87	5.80	4.20	6.04	1.87	3.80	2.20	4.30
14	4.17	6.26	4.53	6.50	2.17	4.26	2.53	4.79
16	4.56	6.84	4.95	7.09	2.56	4.84	2.95	5.43
18	4.93	7.40	5.36	7.67	2.93	5.40	3.36	6.03
19	5.11	7.67	5.55	7.95	3.11	5.67	3.55	6.33
20	5.29	7.94	5.75	8.22	3.29	5.94	3.75	6.62
22.4	5.71	8.56	6.20	8.87	3.71	6.56	4.20	7.29
25	6.14	9.21	6.67	9.55	4.14	7.21	4.67	8.00
28	6.62	9.93	7.19	10.30	4.62	7.93	5.19	8.78
31.5	7.16	10.74	7.78	11.16	5.16	8.74	5.78	9.67
35.5	7.76	11.64	8.42	12.10	5.76	9.64	6.42	10.63
40	8.40	12.60	9.12	13.12	6.40	10.60	7.12	11.68
45	9.09	13.63	9.86	14.22	7.09	11.63	7.86	12.80
50	9.75	14.62	10.58	15.28	7.75	12.62	8.58	13.87

In addition to Table 2, engineers, companies, researchers, etc. may also use Fig. 4 to quickly reference the optimal transmission ratio range. This figure is constructed as a visual support tool for the pre-design stage, helping users select suitable transmission ratios without the need for repeated calculations. Thanks to its concise layout, Fig. 4 can be easily printed together with drawings or design documents, making it convenient to carry to the field or the design workshop. It is particularly useful for quick reference when comparing or adjusting transmission ratio options.

The comparison between the SQP algorithm and the analytical method is illustrated in Fig. 5 and Fig. 6 for the case where the coefficient $K = 1.25, K = 1.6$.

Under practical operating conditions with differing requirements, the gear ratio should be chosen to satisfy the specific objective. Fig. 5 and Fig. 6 provide researchers and manufacturers with a quick reference for objective-based selection. For example, when the aim is simply to ensure uniform strength and oil-bath lubrication, the ratio given by the analytical method is appropriate. By contrast, if

a more compact gearbox is required while still meeting the criteria of uniform strength, oil-bath lubrication, and minimum volume, the optimal gear-ratio range produced by the SQP algorithm is recommended.

To further clarify the influence of the optimization method on the overall geometric size of the gearbox, the volume obtained by the analytical method and by the SQP algorithm is presented as a function of the overall transmission ratio u_h in Fig. 7, Fig. 8, and Fig. 9. The plots are considered for two layout arrangements, including the one in the same plane and the one in the orthogonal plane, corresponding to two values of $K = 1.25$ and $K = 1.6$. In addition to the direct comparison of the volume values, the percentage reduction in volume of SQP relative to the analytical solution is also presented in order to provide a clearer evaluation of the effectiveness of the optimization method.

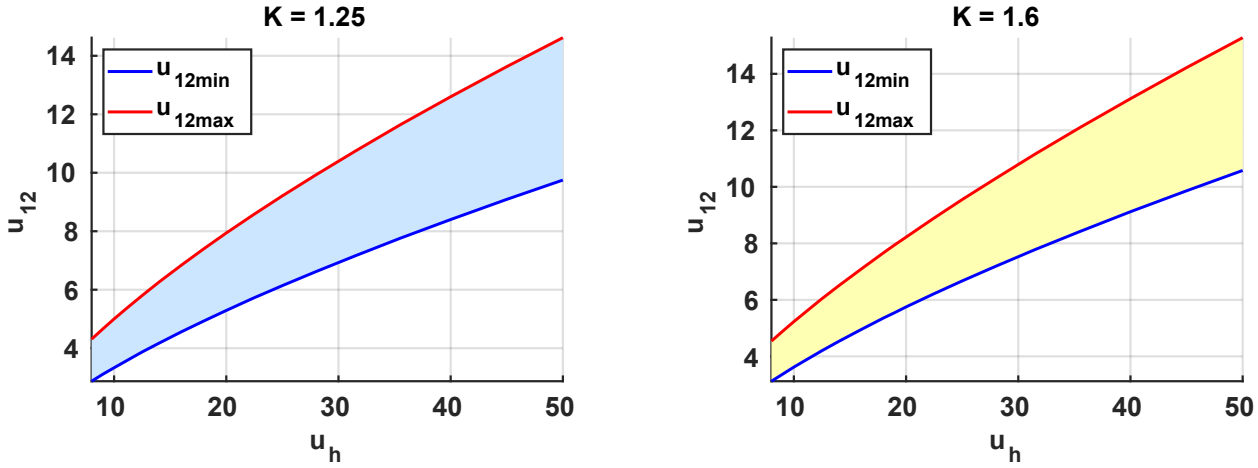

(a) (b)

Fig. 3. Two-stage gearbox with expanded layout in the same plane (a) when $K = 1.25$ and (b) when $K = 1.6$

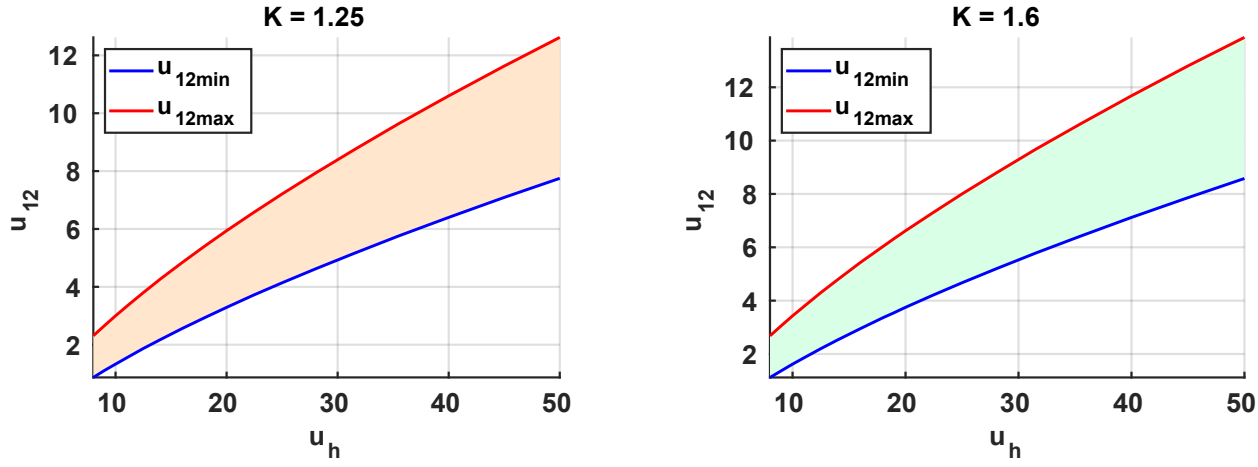

(a) (b)

Fig. 4. Two-stage gearbox with expanded layout in the orthogonal plane (a) when $K = 1.25$ and (b) when $K = 1.6$

Fig. 7 shows that, in the case of the layout in the same plane, the gearbox volume increases monotonically with the overall transmission ratio u_h for both investigated values of K. In all cases, the SQP curve always lies below the analytical curve, indicating that the SQP algorithm always provides a design with a smaller volume. This difference is more pronounced when $K = 1.25$, whereas for $K =$

1.6 the two curves are closer to each other over the entire investigated range. This indicates that, for the layout in the same plane, the analytical method provides results that are fairly close to the optimal solution when K is larger, while SQP still plays the role of refinement to further reduce the gearbox volume.

Fig. 8 shows that, for the layout in the orthogonal plane, the gearbox volume also increases continuously with u_h, following a trend similar to that observed for the layout in the same plane. However, the difference between the SQP curve and the analytical curve is more evident in this case, especially when $K = 1.25$. This result indicates that, for the orthogonal layout, the SQP algorithm exploits the design domain more effectively and provides a more significant reduction in volume than the analytical calculation method. In contrast, when $K = 1.6$, the two characteristic curves become quite close to each other, indicating that the potential for further volume improvement by numerical optimization is no longer as large as in the case of $K = 1.25$.

Fig. 9 shows that the percentage reduction in volume of SQP relative to the analytical solution generally does not vary significantly with u_h, meaning that the effectiveness of the optimization algorithm is maintained rather stably over the entire investigated transmission-ratio range. For the layout in the same plane, the volume reduction is approximately 10% when $K = 1.25$ and about 3% when $K = 1.6$. Meanwhile, for the layout in the orthogonal plane, the volume reduction reaches about 21% when $K = 1.25$ but is only about 2.5–3% when $K = 1.6$. Thus, the volume-reduction efficiency of SQP depends strongly on the layout arrangement and the value of K, in which the case of the orthogonal layout with $K = 1.25$ shows the greatest optimization potential. This result also reinforces the role of the analytical lookup table as an initial guiding tool in the preliminary design stage, while SQP serves as an additional optimization step to further reduce the volume within the feasible solution domain.

Overall, the analytical method and the SQP algorithm show the same trend of volume variation with the overall transmission ratio, but SQP always provides better results in terms of volume reduction. This demonstrates that the lookup table established from the analytical model has high practical value in the initial preliminary design stage, whereas the SQP algorithm is suitable for refinement and for selecting a more optimal solution for each specific configuration.

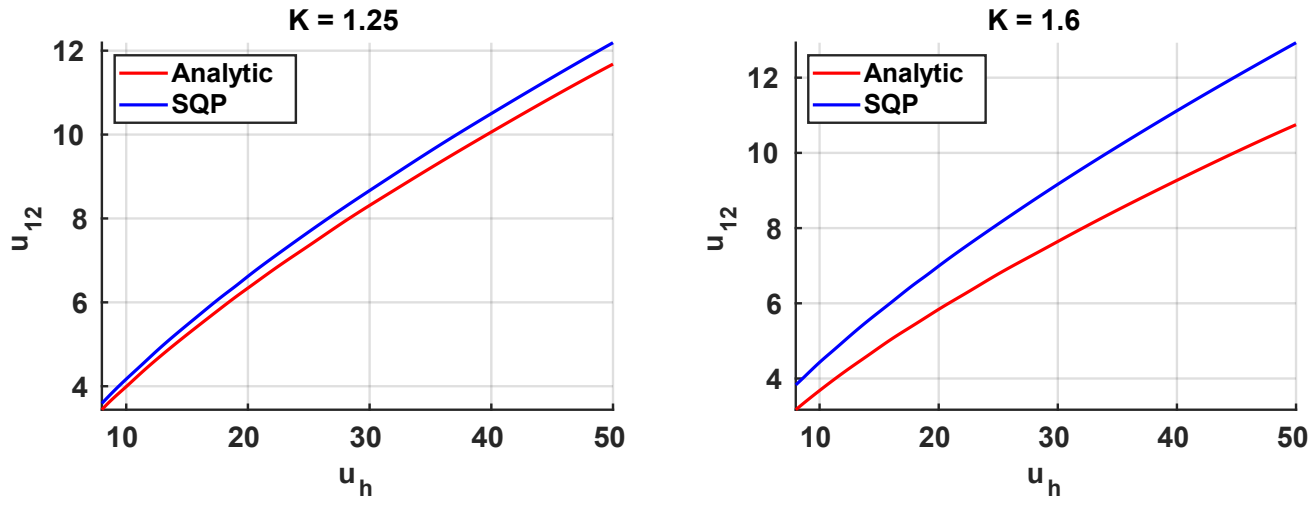

(a) (b)

Fig. 5. Comparison of average u_{12} values for the expanded two-stage gearbox in the same plane at (a) $K = 1.25$ and (b) $K = 1.6$

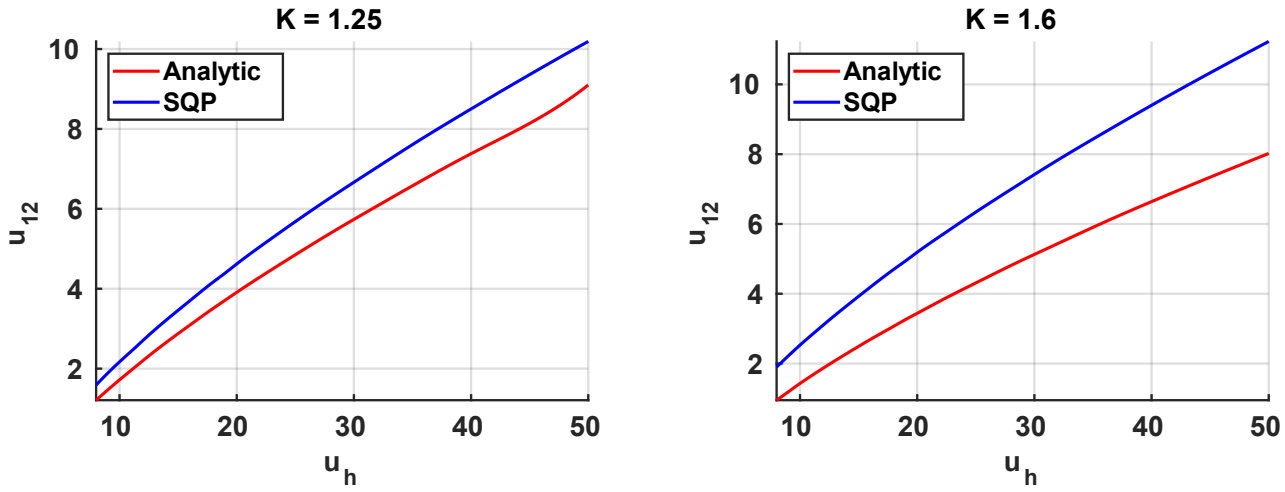

(a) (b)

Fig. 6. Comparison of average u_{12} values for the expanded two-stage gearbox in the orthogonal plane at (a) $K = 1.25$ and (b) $K = 1.6$

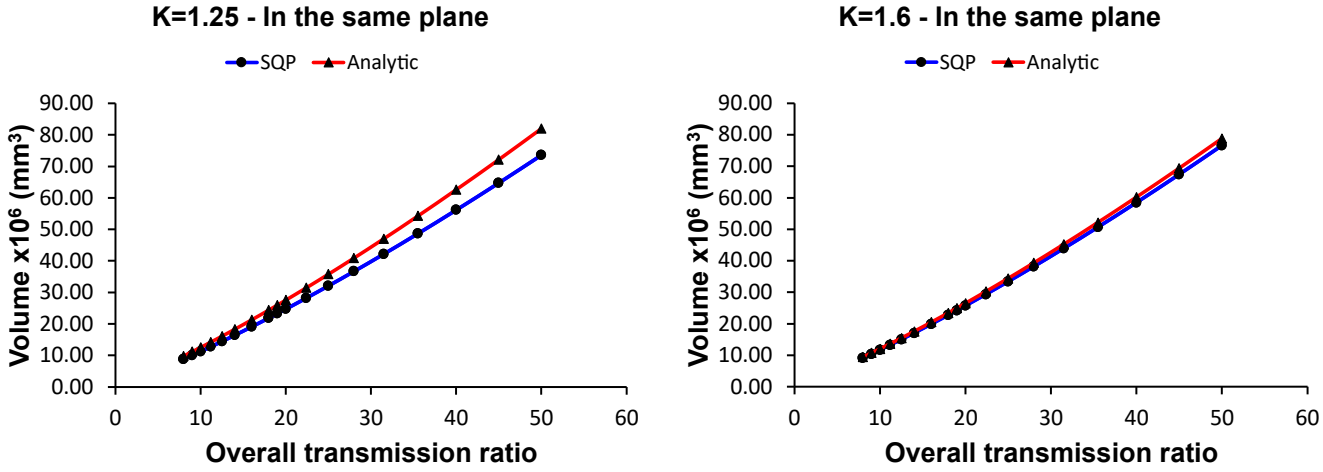

(a) (b)

Fig. 7. Volume of the gearbox in the same plane when (a) $K = 1.25$ and (b) $K = 1.6$

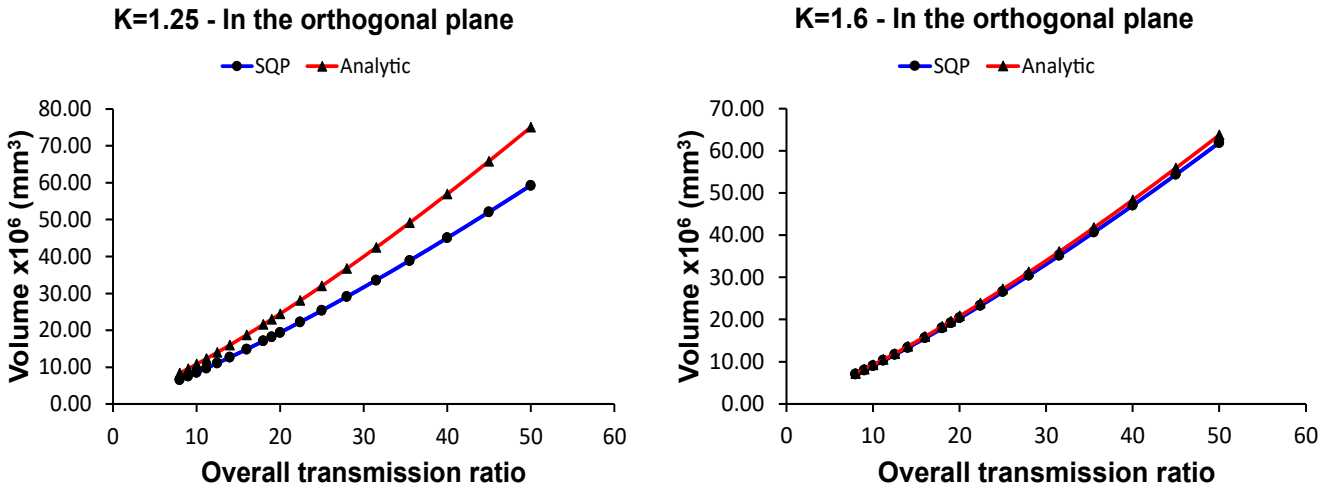

(a) (b)

Fig. 8. Volume of the gearbox in the orthogonal plane (a) $K = 1.25$ and (b) $K = 1.6$

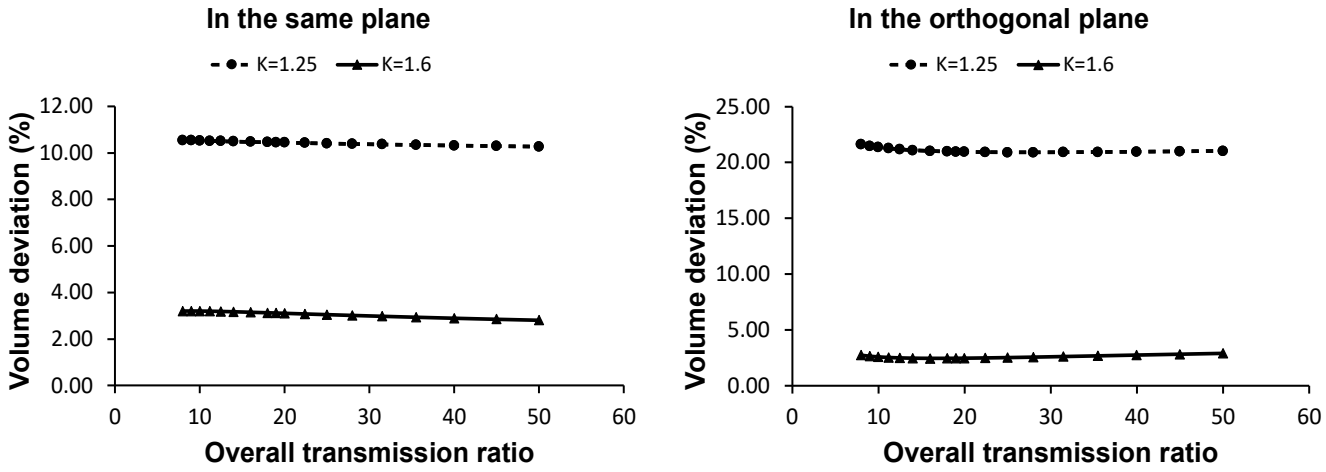

(a) (b)

Fig. 9. Percentage reduction in volume of SQP compared to the analytical method with (a) in the same plane and (b) in the orthogonal plane

Table 3. Two-stage gear transmission parameters

	In the same plane				In the orthogonal plane			
Spur gears	1	2	3	4	1	2	3	4
d_{wi}	54	302	96	342	62	248	81	405
u_{ij}	5.6		3.55		4.0		5.0	
m	2		3		2		3	
a_{wij}	180		225		160		250	
b_{wji}	45		75		40		80	

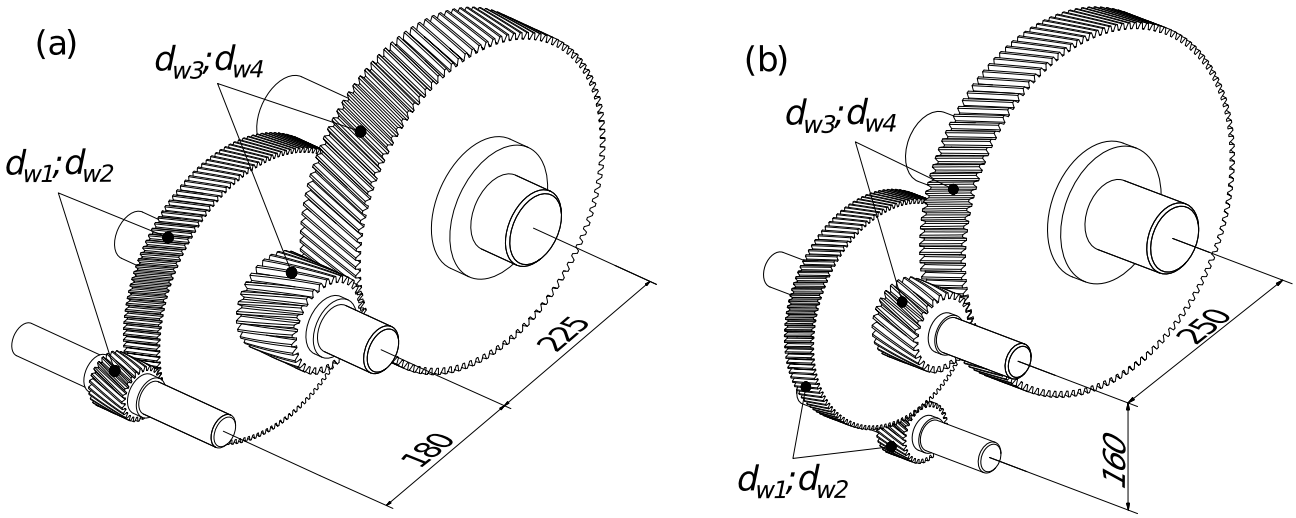

Fig. 10. The two-stage gear is modeled in 3D (a) in the same plane and (b) in the orthogonal plane

4.3. Application to a Practical Problem

The task is to calculate the drivetrain system shown in Fig. 1 using the following given parameters: a motor with a rated power of 4.0 kW and a rotational speed of $n = 1440$ rpm. The gear efficiency is assumed to be equal to the bearing efficiency, both set at 0.98. The coefficients $\psi_{ba12} = 0.25, \psi_{ba34} = 0.315, [\sigma_{H12}] \approx [\sigma_{H34}] \approx 300$ MPa, and the other coefficients are standard values.

Based on Table 2, the following set of parameters is selected: a) In the same plane $u_h = 20, u_{12} = 5.6, u_{34} = 3.55$; b) In the orthogonal plane $u_h = 20, u_{12} = 4, u_{34} = 5$. The results are presented in Table 3 and Fig. 10.

5. Conclusions

This study shows that the lookup table for optimal transmission ratio distribution plays a particularly important role in the pre-design stage of a two-stage gearbox. It not only serves as a rapid reference tool, but also provides an initial quantitative basis for designers to select a rational transmission ratio distribution scheme during the conceptual design phase, while simultaneously ensuring three core requirements: uniform contact strength between gear pairs, appropriate oil-immersion lubrication conditions, and a tendency toward minimizing gearbox volume. As a result, the preliminary design process no longer depends excessively on experience, but is instead supported by a computational framework with a clear analytical and optimization basis. This constitutes the primary practical application of the research, and it also provides a foundation for further development toward detailed design, verification, and model extension to more complex transmission systems in the future.

In addition, formulating the problem in analytical form and solving it by the SQP algorithm shows that the proposed method is capable of effectively handling geometric optimization problems with strict nonlinear constraints. The obtained results not only reflect the variation trend of rational transmission ratio distribution in each configuration, but also clarify the influence of the arrangement scheme and the parameter K on the feasible design domain.

However, this study is mainly significant at the pre-design and preliminary design stages. Factors such as vibration, noise, tooth-root bending stress, manufacturing errors, lubricant oil temperature, and technological conditions have not yet been deeply considered in the current model. Therefore, the proposed lookup table should be regarded as an initial foundation for guiding parameter selection before being further verified and refined through more detailed analytical steps.

In future studies, this method can be extended in many directions to further enhance both its academic value and practical applicability. First, the model can be developed for various types of gearboxes, not only limited to two-stage spur gearboxes, but also extended to multi-stage gearboxes, transmission systems with large transmission ratios, as well as more complex spatial configurations. In addition, this approach can also be applied to various types of drives such as bevel gears, worm gear sets, bevel gears, and planetary gear trains, thereby establishing lookup tables and optimal transmission ratio distribution laws suitable for each type of transmission system.

Moreover, future research may integrate additional optimization objectives such as bending strength, vibration, noise, transmission efficiency, power loss, lubricant oil temperature, and system service life, which would enable the model to approach actual operating conditions more closely. At that stage, the lookup table would no longer be only a geometric pre-design support tool, but could also become a basis for initial parameter selection under multi-objective optimization and multiple operating conditions.

In particular, combining the optimization model with modern simulation tools such as finite element analysis (FEA) and computational fluid dynamics (CFD) is a highly promising development direction. FEA can be used to further evaluate stress, deformation, stiffness, vibration, and fatigue strength of the transmission system, while CFD allows detailed analysis of the lubrication process, oil flow distribution, heat dissipation capability, and churning losses in the gearbox. This combination will help verify and calibrate the optimal results obtained from the analytical model, while also improving design accuracy and shortening product development time.

In the long term, the proposed method can be integrated into modern digital design processes to support the automation of parameter selection for mechanical transmission systems. When combined with multi-objective optimization algorithms, standard databases, machine learning models, and CAE simulation software, this research direction has the potential to establish an intelligent design framework for various types of gearboxes and gear transmission systems, thereby better satisfying the increasingly demanding industrial requirements for compactness, strength, efficiency, and reliability.

Acknowledgement

We acknowledge the support of time and facilities from Ho Chi Minh City University of Technology (HCMUT), VNU-HCM for this study.

References

[1] N.S. Sanoussi, T. Belgasam, M. Hammami, M.S. Abbes, Z. Xue, O. Mande. (2026). Machine Learning–Based Optimization of Frictional Power Losses in Spur-Geared Transmissions. *Journal of Mechanical Design*, 148(3), 033501. https://doi.org/10.1115/1.4070619

[2] X. Yu, B. Tang, K. Zhang. (2021) Fault Diagnosis of Wind Turbine Gearbox Using a Novel Method of Fast Deep Graph Convolutional Networks. *IEEE Transactions on Instrumentation and Measurement,* 70, 6502714, pp. 1-14. https://doi.org/10.1109/TIM.2020.3048799

[3] G. He, Y. Feng, B. Jiang, H. Wu, Z. Wang, H. Zhao, Y. Liu. (2023). Corrosion and abrasion behavior of high-temperature carburized 20MnCr5 gear steel with Nb and B microalloying. *Journal of Materials Research and Technology*, 25, 5845–5854. https://doi.org/10.1016/j.jmrt.2023.07.048

[4] D.-B. Vu, H.-D. Tran, V.-T. Dinh, D. Vu, N.-P. Vu, V.-T. Nguyen. (2024). Solving a Multi-Objective Optimization Problem of a Two-Stage Helical Gearbox with Second-Stage Double Gear Sets Using the MAIRCA Method. *Applied Sciences,* 14(12), 5274. https://doi.org/10.3390/app14125274

[5] C. Gologlu, M. Zeyveli. (2009). A genetic approach to automate preliminary design of gear drives. *Computers & Industrial Engineering*, 57(3), 1043–1051. https://doi.org/10.1016/j.cie.2009.04.006

[6] R.C. Sanghvi, A.S. Vashi, H.P. Patolia, R.G. Jivani. (2014). Multi-Objective Optimization of Two-Stage Helical Gear Train Using NSGA-II. *Journal of Optimization*, 2014, 670297. https://doi.org/10.1155/2014/670297

[7] O. Buiga, L. Tudose. (2014). Optimal mass minimization design of a two-stage coaxial helical speed reducer with Genetic Algorithms. *Advances in Engineering Software*, 68, 25–32. https://doi.org/10.1016/j.advengsoft.2013.11.002

[8] Y. Yamanaka, S. Wakahara, K. Yoshida. (2024). Simultaneous Design of Two-stage Gearboxes —An Application of Gravitational Particle Swarm Algorithm. *Transactions of the Institute of Systems, Control and Information Engineers*, 37(6), 158–166. https://doi.org/10.5687/iscie.37.158

[9] K. Deb, S. Jain. (2003). Multi-Speed Gearbox Design Using Multi-Objective Evolutionary Algorithms. *ASME Journal of Mechanical Design,* 125(3), 609-619. https://doi.org/10.1115/1.1596242

[10] S. Kim, S. Moon, J. Sohn, Y. Park, C. Choi, G. Lee. (2020). Macro geometry optimization of a helical gear pair for mass, efficiency, and transmission error. *Mechanism and Machine Theory*, 144, 103634. https://doi.org/10.1016/j.mechmachtheory.2019.103634

[11] S. Kim, S. Moon, C. Choi, J. Sohn. (2025). Optimal design strategy for gear pairs integrating macro and micro geometry optimization. *Mechanism and Machine Theory*, 214, 106119.

https://doi.org/10.1016/j.mechmachtheory.2025.106119

[12] C. Kalligeros, C. Papalexis, G. Kostopoulos, K. Terpos, P. Tzouganakis, K. Kostas, D. Halim, J. Yang, C. Spitas, A. Tsolakis, E. Sakaridis, V. Spitas. (2026). A multi-objective macro-geometry spur gear optimization process to improve weight, efficiency and NVH performance utilizing neural networks. *Mechanism and Machine Theory*, 223, 106422. https://doi.org/10.1016/j.mechmachtheory.2026.106422

[13] L. Tudose, O. Buiga, C. Ştefanache, A. Sóbester. (2010). Automated optimal design of a two-stage helical gear reducer. *Structural and Multidisciplinary Optimization*, 42, 429–435. https://doi.org/10.1007/s00158-010-0504-z

[14] B. Karmi, A. Saouab, A. Guerine, S. Bouaziz, A. El Hami, M. Haddar, K. Dammak. (2024). Reliability based design optimization of a two-stage wind turbine gearbox. *Mechanics & Industry*, 25, 16. https://doi.org/10.1051/meca/2024010

[15] M. Patil, P. Ramkumar, K. Shankar. (2019). Multi-objective optimization of the two-stage helical gearbox with tribological constraints. *Mechanism and Machine Theory*, 138, 38–57. https://doi.org/10.1016/j.mechmachtheory.2019.03.037

[16] M.B. Sánchez, M. Pleguezuelos, J.I. Pedrero. (2019). Strength model for bending and pitting calculations of internal spur gears. *Mechanism and Machine Theory*, 133, 691–705.https://doi.org/10.1016/j.mechmachtheory.2018.12.016

[17] S. Wang, A. Xieeryazidan, X. Zhang, J. Zhou. (2020). An Improved Computational Method for Vibration Response and Radiation Noise Analysis of Two-Stage Gearbox. *IEEE Access*, 8, 85973–85988. https://doi.org/10.1109/ACCESS.2020.2990938

[18] J. Kattelus, J. Miettinen, A. Lehtovaara. (2018). Detection of gear pitting failure progression with on-line particle monitoring. *Tribology International*, 118, 458–464. https://doi.org/10.1016/j.triboint.2017.02.045

[19] International Organization for Standardization. (2006). ISO 6336-2:2006 Calculation of load capacity of spur and helical gears - Part 2: Calculation of surface durability (pitting).

[20] American Gear Manufacturers Association. (2025). ANSI/AGMA 2101-E25 Fundamental Rating Factors and Calculation Methods for Involute Spur and Helical Gear Teeth.

[21] German Institute for Standardization. (1987). DIN 3990-2:1987-12 Calculation of load capacity cylindrical gears; calculation of pitting resistance.

[22] K.-H. Grote, E.K. Antonsson. (2009). Springer Handbook of Mechanical Engineering. *Springer*. https://doi.org/10.1007/978-3-540-30738-9

[23] D.H. Huynh, L.H. Nguyen. (2025). Optimization of transmission ratios in a three-stage spur-helical gearbox using an analytical sizing algorithm and differential evolution. *Results in Engineering*, 28, 108080. https://doi.org/10.1016/j.rineng.2025.108080

[24] S. Maláková, S. Sivák. (2022). Practical Example of Modification of a Gearbox Lubrication System. *Lubricants*, 10(6), 110. https://doi.org/10.3390/lubricants10060110

[25] E. Ben Younes, E. Rigaud, J. Perret-Liaudet, J. Bruyère, C. Changenet. (2024). Optimization of energy efficiency and NVH behaviour of a helical gear unit. *Mechanics & Industry*, 25, 1. https://doi.org/10.1051/meca/2023042

[26] H. Liu, T. Jurkschat, T. Lohner, K. Stahl. (2017). Determination of oil distribution and churning power loss of gearboxes by finite volume CFD method. *Tribology International*, 109, 346–354.

https://doi.org/10.1016/j.triboint.2016.12.042

[27] M. Bozca. (2018). Transmission error model-based optimisation of the geometric design parameters of an automotive transmission gearbox to reduce gear-rattle noise. *Applied Acoustics*, 130, 247–259. https://doi.org/10.1016/j.apacoust.2017.10.005

[28] Z.B. Xu, J.Q. Min. (2013). Sequential Quadratic Programming Design of Gear Transmission. *Applied Mechanics and Materials*, 437, 481–484. https://doi.org/10.4028/www.scientific.net/AMM.437.481

[29] E. Chaturvedi, P. Acar, C. Sandu. (2023). Multi-objective macrogeometry optimization of gears: Comparison between sequential quadratic programing and genetic algorithm. *Mechanics Based Design of Structures and Machines*, 51(1), 97–112. https://doi.org/10.1080/15397734.2022.2146710

[30] M.A. Elsiedy, H.A. Hegazi, A.M. El-Kassas, A.A. Zayed. (2024). Multi-objective design optimization of polymer spur gears using a hybrid approach. *Journal of Engineering and Applied Science*, 71, 105. https://doi.org/10.1186/s44147-024-00443-5

[31] V. Bhandari. (2014). Machine design data book. *McGraw-Hill Education*.